given in terms of phase shifts, η_l, by

$$\sigma(\theta)=\frac{1}{4k^2}\left|\sum_{l=0}^{\infty}(2l+1)(e^{2i\eta l}-1)P_l(\cos\theta)\right|^2. \quad \text{(A-1)}$$

In integrating over a right circular cone whose axis lies in the equatorial plane of the scattering sphere and which has a half-apex-angle $\pi/4$, the cross section Q_A will be given by

$$Q_A=\int_{\pi/4}^{3\pi/4}\sigma(\theta)\sin\theta\phi(\theta)d\theta, \quad \text{(A-2)}$$

where

$$\phi(\theta)=\cos^{-1}(\cot^2\theta). \quad \text{(A-3)}$$

On expansion of Eq. (A-1) and integration, the interference terms vanish because of the symmetry of the integration limits around the equator of the scattering sphere, leaving

$$Q_A=(1/k^2)(I_0\sin^2\eta_0+9I_1\sin^2\eta_1+\cdots), \quad \text{(A-4)}$$

where

$$I_n=\int_{\pi/4}^{3\pi/4}(\cos\theta)^{2n}\sin\theta\cos^{-1}(\cot^2\theta)d\theta. \quad \text{(A-5)}$$

After integration by parts to eliminate the arccosine from the integrand, changing variables by

$$\cos\theta=(1/\sqrt{2})\sin(\psi/2) \quad \text{(A-6)}$$

and by $z=e^{i\psi}$ transforms the integrals to

$$I_n=\frac{1}{2n+1}\frac{(-1)^{n+1}}{2^{3n+1/2}}\times\frac{1}{i}\oint\frac{(z-1)^{2n+2}}{z^{n+1}(z^2+6z+1)}dz, \quad \text{(A-7)}$$

where the integration is taken about the unit circle in the complex plane. Evaluation of the residues at the two poles inside the unit circle yields

$$\begin{aligned}I_0&=2\pi[1-(1/\sqrt{2})],\\ I_1&=\pi/3[2-(5/2\sqrt{2})].\end{aligned} \quad \text{(A-8)}$$

Substituting (A-8) into (A-4) and recalling that the total partial cross sections are given by

$$\begin{aligned}Q_0&=(4\pi/k^2)\sin^2\eta_0,\\ Q_1&=(4\pi/k^2)3\sin^2\eta_1,\end{aligned}$$

yields Eq. (7) immediately.

The analytical evaluation of the cross section for scattering into a right circular cone of *any* apex angle whose axis lies in the equatorial plane of the scattering sphere may be carried out similarly.

PHYSICAL REVIEW VOLUME 112, NUMBER 4 NOVEMBER 15, 1958

Charge Exchange in Proton-Hydrogen-Atom Collisions*

WADE L. FITE, R. THEODORE BRACKMANN, AND WILLIAM R. SNOW
John Jay Hopkins Laboratory for Pure and Applied Science, General Atomic Division of General Dynamics Corporation, San Diego, California

(Received July 28, 1958)

The charge-exchange cross sections for the reactions $p+H\rightarrow H+p$, and $H_2^++H\rightarrow H_2+p$ have been examined over the energy range 200 to 14 000 ev. In the experiment a dc fast-ion beam crossed a slow atomic hydrogen beam which was chopped at 100 cps. The desired signal thus was separable from the much larger signal arising from interaction of the ions with the residual gas in the vacuum chamber, because the signal arising from the interaction of the two beams occurred at the chopping frequency and in a specified phase. The signals used were the saturated slow-ion currents, recorded at a detector which did not discriminate the ion mass, and the slow-ion currents after mass analysis. The measured values at high energies agree very satisfactorily with the Born approximation calculations by Bates and Dalgarno and, at low energies, with calculations by Dalgarno and Yadav using the method of perturbed stationary states. Experimental comparison of cross sections for proton and deuteron collisions is presented.

I. INTRODUCTION

As a target system in a collision experiment, the free hydrogen atom possesses the virtue that its wave functions are completely and exactly known. Thus, in the theoretical treatment of a collision between the hydrogen atom and any elementary particle, the only error which can arise occurs through the intrinsic failure of the particular scattering approximation used in the theory. As a result, comparison of a theoretical prediction with experimental results of scattering cross-section measurements for those collisions in which the hydrogen atom is the target serves to evaluate the validity and degree of failure of the scattering approximation only.

In addition to this basic interest, collision cross sections of the hydrogen atom (or deuterium atom, since the extranuclear properties are virtually identical) are of importance in understanding the operation of experimental controlled thermonuclear devices, es-

* This research was supported by the joint General Atomic—Texas Atomic Energy Research Foundation Controlled Fusion Project.

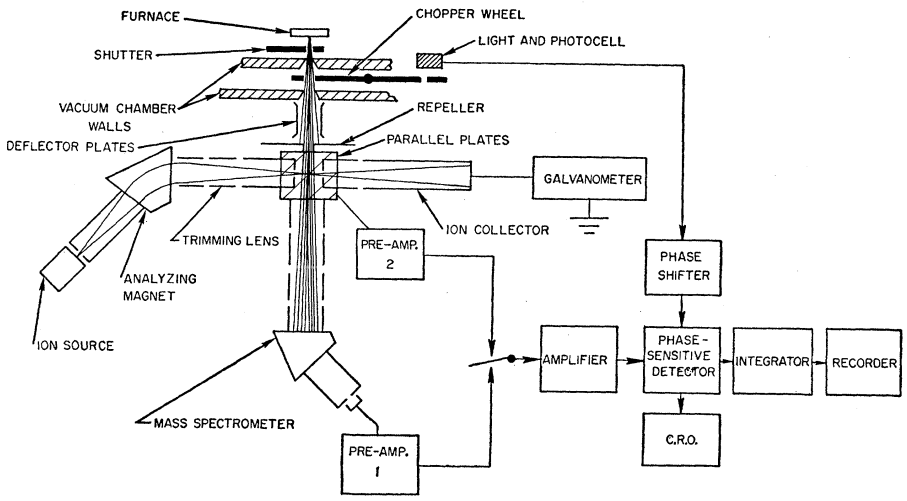

FIG. 1. Schematic diagram of experimental arrangement.

pecially in their early heating stages. In this connection the charge-exchange cross sections discussed in this paper are perhaps especially important, for through charge exchange fast ions in a thermonuclear device can become neutralized and escape any "electromagnetic bottle."

For these reasons, as well as to understand better certain astrophysical and auroral processes, the collisions between protons and hydrogen atoms are perhaps the most interesting of the inelastic atomic collisions of heavy particles.

In the present experiments, as in usual charge-exchange measurements, data were to be derived from the appearance of free electrons and slow ions resulting from the collision of fast ions with slow neutral atoms and molecules.[1]

II. EXPERIMENTAL APPROACH

A schematic diagram of the modulated atomic beam apparatus used in the present experiments is shown in Fig. 1. The atom beam proceeded from a tungsten furnace in the first of three differentially pumped vacuum chambers, into the second vacuum chamber where the beam was modulated at 100 cps by a mechanical chopping wheel, and thence into the third vacuum chamber. As the beam proceeded into the third chamber, it first passed between a pair of parallel deflecting plates used to remove electrons and ions coming from the furnace and accompanying the atoms in the beam, after which the atom beam was crossed by a dc ion beam. With this arrangement, any signal caused from interactions of ions and the residual gas in the vacuum chamber was a dc signal (plus noise), whereas the signal arising from the interactions of the ions with atoms in the beam was identifiable by its occurring at the modulation frequency and in a specified phase. The circuitry and general experimental features of our atomic beam apparatus have been described previously.[2–4]

The ion beam was produced in an electron bombardment source, which is a simplification of the type of source described by Finkelstein.[5] It was normally operated as a hot-cathode arc discharge through a mixture of hydrogen gas and water vapor. The ion beam was magnetically analyzed by a 45° deflection magnet. For simplicity, the plane of the ion orbit was rotated 90° for representation in the schematic diagram. The analyzing magnet was actually placed so that the direction of the magnetic field was parallel to the atomic beam machine's axis, along which the beam proceeded, so that the sector magnet alone tended to focus the ion beam into a line image coincident with the atomic beam. In addition, two electrostatic focusing devices were used for the ion beam. The first was a "cylinder lens" (not shown in the schematic), placed between the ion source and the analyzing magnet, which focused the beam into a line image at the same position as, but perpendicular to, the magnetic focusing image. Thus, the actual ion-beam shape was, at the point of intersection of the two beams, more a point than a line. The second lens—the trimming lens shown in the schematic diagram—was sometimes used to increase ion current, at the cost of ion-energy resolution, by focusing into the first aperture ions which would otherwise have been excluded because of their energy. The first aperture was made small enough and placed so as to ensure that all ions leaving the aperture would have to traverse the atomic beam. With the trimming lens in use, the energy

[1] For a general discussion of charge exchange and scattering of ions by atoms and molecules, see H. S. W. Massey and E. H. S. Burhop, *Electronic and Ionic Impact Phenomena* (Clarendon Press, Oxford, 1952), Chap. 8.

[2] W. L. Fite and R. T. Brackmann, this issue [Phys. Rev. **112**, 1141 (1958)].

[3] W. L. Fite and R. T. Brackmann, this issue [Phys. Rev. **112**, 1151 (1958)].

[4] Brackmann, Fite, and Neynaber, preceding paper [Phys. Rev. **112**, 1157 (1958)].

[5] A. T. Finkelstein, Rev. Sci. Instr. **11**, 94 (1940).

spread, as determined from stopping potentials, was about 10% of the ion energy at energies less than 1000 ev, and above this value the energy spread was about 90 ev. At the higher energies, the spread was determined by the fields in the electron-bombardment ion source. Without its use, the ion-energy spread, at energies less than 2000 ev, was about 4% of the ion energy, and less at higher energies.

The second aperture was made smaller than the height of the atomic beam, so that when no current was recorded to this aperture, it was ensured that all current to the ion collector had indeed traversed the atomic beam. In practice, less than 1% of the total ion current was recorded at the second aperture. The ion collector was made deep and electrically biased to suppress secondary electron emission, and was enclosed by a shield to prevent collection of ions and electrons formed in the background gas.

Installed within the ion collector was a tungsten filament (not shown on the schematic diagram) for the production of an electron beam which crossed the atomic beam in the direction opposite to that of the ion beam. This beam was used to mass-monitor the particles in the neutral beam under any set of furnace operating conditions. Since the cross sections for ionization on electron impact of both H and H_2 are known,[2] mass spectrometer signals gave direct measures at any time of the relative number densities of atoms and molecules in the neutral beam.

Two signals were used in measuring the numbers of slow ions produced in the collisions of fast ions and the slow neutral particles. The first was the current to the various mass peaks in the mass spectrometer. This instrument operated exactly as previously described[2] when either the ion or electron beam produced the slow ions. Not only were relative cross sections at various ion energies for production of slow ions directly measurable, but also the various species produced by the interactions of ions and neutral species were ascertainable.

The second signal was the saturated current at the modulation frequency which arrived at the lower one of a pair of parallel plates located immediately above and below the region of interaction of the atom and ion beams, when electric fields were placed so as to draw all particles of a given sign of charge to the lower plate.

These plates were operated in the same basic manner used by other investigators in the measurement of charge exchange.[6,7] With parallel plates biased to receive saturated positive and negative currents, addition of these currents will automatically cancel both the current contributions of ionization on ion impact and secondary electron emission by ion impact at the negative plate, leaving only the true charge-exchange current. Rather than simultaneously measuring these currents, we planned the present experiments to resemble those of Keene,[7] where the plates were biased first in one direction and then in the other and the measured signals at one of the plates were combined mathematically. Adding the two currents electrically, as was done by Hasted,[6] was precluded by signal-to-noise considerations. This subject will be discussed later.

One simplification was possible in the use of these plates in the present experiments as compared to the more usual charge-exchange experiment. With crossed beams, the source of the slow ions resulting from charge exchange is a very small region of space—essentially a point source rather than the usual line source formed where an ion beam is passed through a gas. Thus, the use of guard rings, etc., was not necessary in the determination of the path length over which the ions were formed; the path length was given by the neutral-beam geometry. Actually, in measurements of the proton-hydrogen-atom cross sections, even this information was not required, for the direct physical measurable was the ratio of the cross sections of the hydrogen atom and the hydrogen molecule. The absolute atomic cross sections were determined from knowledge of the molecular cross sections. The only requirement on geometry was that it should be constant and independent of the relative numbers of atoms and molecules in the neutral beam.

The cross sections for the appearance of slow ions were measured with both the mass spectrometer and the parallel plates. However, because of the intrinsic capability of the plates to determine only the charge-exchange component of the ion current, the primary data were obtained with the parallel plates. The mass spectrometer was used to provide a check on these results, to mass-monitor the neutral beam through ionization on electron impact, and to ascertain the species of ions resulting from any given ion-atom or ion-molecule collision.

The signals from the preamplifier of either the parallel plates or the mass spectrometer were treated in the manner previously described in reference 2.

III. DETERMINATION OF ABSOLUTE CROSS SECTIONS

As in our earlier work,[2–4] the approach used to determine absolute charge-exchange cross sections was to measure the ratio of the cross sections of the hydrogen atom and the hydrogen molecule at a given ion energy and then multiply the ratio by the absolute molecular cross section determined by other investigators. As an alternate approach, curves of relative cross section, requiring normalization at any one energy, were taken.

In measuring the ratio of cross sections, advantage was taken of the facts that (1) apparently complete thermal equilibrium was achieved in the furnace, and (2) the amount of mass flow per unit time in the beam was constant and independent of both the furnace

[6] J. B. Hasted and J. B. H. Stedeford, Proc. Roy. Soc. (London) A227, 466 (1955).
[7] J. P. Keene, Phil. Mag. 40, 369 (1949).

temperature and degree of dissociation in the furnace under the experimental conditions. (The reader is referred to reference 1 in regard to these statements as well as for further details of the present arguments.) Under these circumstances, it is convenient to define $S_0(T)$ as the signal per unit current of a specific ion of a given energy, which would have been observed with the furnace at the absolute temperature, T, *if the hydrogen molecules had not dissociated.* Defining a reference furnace temperature, T_r, which is sufficiently low that the beam is a pure molecular beam, the signal per unit ion current (of the same ion at the same energy), S_r, is related to $S_0(T)$ by

$$S_0(T)=(T_r/T)^{\frac{1}{2}}S_r. \tag{1}$$

This equation arises because the signal in a collision process is proportional to number density of particles in the neutral beam, which, for fixed mass flow, decreases linearly with the particle speed and therefore with the square root of the absolute temperature. [The prediction of Eq. (1) that $ST^{\frac{1}{2}}$ should be constant at temperatures below which dissociation occurs was again verified by using the heavy-particle collisions.]

At furnace temperatures at which the hydrogen gas is partially dissociated, the signal per unit ion current, S_2, arising from collision of the ions with molecules in the neutral beam is given by

$$S_2(T)=(1-D)S_0(T)=(1-D)(T_r/T)^{\frac{1}{2}}S_r. \tag{2}$$

Similarly, the contribution to signal per unit ion current arising from the atoms in the neutral beam is

$$S_1(T)=\frac{Q_1}{Q_2}\frac{2D}{\sqrt{2}}S_0(T)=\sqrt{2}D\left(\frac{T_r}{T}\right)^{\frac{1}{2}}\frac{Q_1}{Q_2}S_r. \tag{3}$$

In these equations, D is the dissociation fraction, defined by Eq. (2), and Q_1/Q_2 is the ratio of the atomic and molecular cross sections for the processes leading to the observed signal. In Eq. (3), the 2 in the numerator arises because the molecule dissociates into two atoms, and the square root of 2 in the denominator comes from the fact that the atom is lighter than the molecule and moves faster by this fraction, therefore remaining in the region of interaction of the ion and neutral beams for a shorter time.

When parallel plates are used to detect the production of all slow ions formed in the collisions, the signal is given by

$$S=S_1+S_2=S_r\left(\frac{T_r}{T}\right)^{\frac{1}{2}}\left(\sqrt{2}D\frac{Q_1}{Q_2}+1-D\right), \tag{4}$$

or

$$S=S_1\left[1+\frac{Q_2}{Q_1}\left(\frac{1-D}{\sqrt{2}D}\right)\right]. \tag{5}$$

The dissociation fraction, D, is determined from comparing peak intensities with the mass spectrometer when the neutral beam is crossed by the electron beam (the gun for which was built into the ion collector) by using the formula

$$D=1\Big/\left(1+\sqrt{2}\frac{Q_1{}^i}{Q_2{}^i}\frac{S_2{}^i}{S_1{}^i}\right), \tag{6}$$

where $S_1{}^i$ and $S_2{}^i$ are atomic and molecular peak strengths on the mass spectrometer, and $Q_1{}^i/Q_2{}^i$ is the ratio of cross sections for ionization of the atom and molecule, as determined in the measurements described in reference 2.

Equation (4) was used to evaluate Q_1/Q_2. For the experiments described here, the usual procedure was to work only at room temperature and around 2700°K with the furnace pressure such that at this higher temperature, D was greater than 0.96. Only spot checks were made for values of Q_1/Q_2 over a range of dissociation fractions. Since, as the results presented later indicate, $Q_1/Q_2\gtrsim 1$, for charge exchange, the total molecular contribution to signals at high furnace temperatures was about 3% or less, as is evident from Eq. (5).

When the mass spectrometer was used in making the measurement of the ratio of cross sections, the mass spectrometer peak heights for both the slow protons and slow $H_2{}^+$ ions were measured. Since both S_1 and S_2 were directly measurable, to obtain Q_1/Q_2, the dissociation fraction was eliminated between Eqs. (2) and (3).

To this point, the derivation of the appropriate equations has been simplified to the case where a single type of ion collides with both atoms and molecules. Actually, in the present experiments there were four charge-exchange reactions of interest, and it is convenient to think of all four simultaneously. The four reactions are

$$p+\mathrm{H}\rightarrow \mathrm{H}+p, \tag{1,1}$$

$$p+\mathrm{H_2}\rightarrow \mathrm{H}+\mathrm{H_2}{}^+, \tag{1,2}$$

$$\mathrm{H_2}{}^++\mathrm{H}\rightarrow \mathrm{H_2}+p, \tag{2,1}$$

$$\mathrm{H_2}{}^++\mathrm{H_2}\rightarrow \mathrm{H_2}+\mathrm{H_2}{}^+. \tag{2,2}$$

It is straightforward to derive the relationships for the ratio of any pair of cross sections in terms of measurable signals with either mass spectrometric detection or nondiscriminating slow-ion detection being used in a manner similar to that described above.

In principle, either of the previously measured (1,2) or (2,2) reactions or both can be used to calibrate all cross sections. In practice, however, the (2,2) reaction is not satisfactory; the various investigators of this cross section are in fairly wide disagreement as to its values. For example, in the vicinity of 1800 ev, where the measurements of Wolf,[8] Hasted,[6,9] Stedeford,[6] and

[8] F. Wolf, Ann. Physik **29**, 33 (1937) (cited by Hasted in reference 6).

[9] H. B. Gilbody and J. B. Hasted, Proc. Roy. Soc. (London) **A238**, 334 (1956).

Keene[7] overlap, values of the charge-exchange cross section between H_2^+ and H_2 range from 6.5 to 9.0×10^{-16} cm^2. It is not obvious whose value is best.

In the case of the (1,2) reaction, these four investigators are in much less disagreement where their energy values overlap. At lower energies Wolf and Hasted are in close agreement and at higher energies Keene and Stedeford do not seriously disagree, nor do they disagree seriously with Whittier[10] or Stier and Barnett.[11] We have somewhat arbitrarily chosen the primary calibration point as 1800 ev, where Wolf's, Hasted's, Stedeford's, and Keene's values range from about 7×10^{-16} to 8×10^{-16} cm^2, and have adopted the value 7.3×10^{-16} cm^2 for the charge-exchange cross section at this point. Although at other energies absolute calibrations to the (1,2) reaction cross section were made, our primary data at other energies have been based upon measurements of relative cross section.

Since the primary data were taken with the parallel plates, when saturated currents of *all* slow ions were measured, two additional points must be considered. The first matter is the species of slow ion formed as a result of the collision. In this regard, mass analysis of the slow ions was made with the mass spectrometer. (Of course, only the ac component of ion current was of interest since only this type of current resulted from interactions of the crossed ion and neutral beams.) Using the four possible combinations of protons and molecular ions colliding with both atoms and molecules, both slow protons and slow molecular ions were recorded. This analysis was made at different energies of the incident ions. In all cases except one the resultant ion *not* expected on the basis of pure charge exchange was not observable above the noise level. The one case was the appearance of slow protons in the (2,2) reaction at 600 ev where the slow-proton current was 2.5% of the slow molecular ion current. On the other hand, the noise level generally was such that unexpected ion current of less than 3 to 5% of the expected ion current could have escaped notice. Consequently, we cannot guarantee that any more than 95 to 97% of the slow ions formed were those predicted in the four charge-exchange reactions given above.

The second matter in regard to the detection schemes used here is ionization of an atom or molecule on ion impact. The mass spectrometer can be used only to detect slow ions and not to determine whether they were formed through a charge exchange or an ionization process. The intrinsic advantage of using nondiscriminating detection of the saturated current at a plate is as follows: When the signal from all slow ions is measured first and then the various electrodes are biased oppositely so that only the electron current from ionizing collisions is measured, subtraction of the magnitudes of two signals (or adding them, maintaining signs of charge) yields only the charge-exchange currents. If the secondary electron emission properties of all electrodes are identical, this procedure also automatically eliminates the very small effects of secondary electron emission due to ion impact at the negatively biased electrodes.

In the present measurements, attempts were made to observe the appearance of ionization electrons in the ion-atom collisions and secondary electrons, but in all instances no signal was discernible above the noise level. Consequently, in the handling of data, no subtraction of electron signal from ion signal was made to separate charge exchange from ionization effects. It is appropriate to comment that the actual noise levels in detection of electrons were higher than in detection of slow ions, and from the measured noise levels, upper limits on the ionization cross sections may be set. For both the $p+H$ and $H_2^+ + H$ collisions, we believe that 2×10^{-16} cm^2 is a very generous figure for upper-limit values over the energy range up to 10 kev. The Born approximation calculations of Bates and Griffing[12] appear to agree with this statement, although their calculated ionization cross-section values above 15 or 20 kev slightly exceed 2×10^{-16} cm^2.

The noise associated with the collection of electrons was found to be several times higher than that associated with the collection of positive ions. With the biases set so that electrons were drawn to the plate, a large dc electron current was found from which, unquestionably, came the noise. The dc electron current is believed to have originated through secondary emission as the fast-ion beam struck the two apertures indicated in the schematic in Fig. 1. Since the observed electron current was too large to have come from the 1% or less of the ion current which struck the second aperture, the major portion of the electron current must have come from the collimating aperture, probably from the side away from the neutral beam where large ion-beam currents were recorded. The electric field penetrating the aperture was adequate to draw slow secondary electrons to the collecting plate in the quantity required to explain the observed dc electron current.

Because of our inability to observe the appearance either of unexpected ions in the mass spectrometer, or of electrons produced in ionizing collisions and secondary emission on ion impact at ion-collecting surfaces, we have treated the appearance of slow ions as being due solely to the charge-exchange process where the resultant slow ion is of the type expected in the four reactions under study. This procedure will tend to make our results high by an amount which is less than 3×10^{-16} cm^2 at low energies, and less than 2×10^{-16} cm^2 at high energies. As is evident from the results to be presented, these indeterminable systematic errors constitute only a small percentage decrease in the

[10] A. C. Whittier, Can. J. Phys. **32**, 275 (1954).
[11] P. M. Stier and C. F. Barnett, Phys. Rev. **103**, 896, (1956).
[12] D. R. Bates and G. W. Griffing, Proc. Phys. Soc. (London) **A66**, 961 (1953).

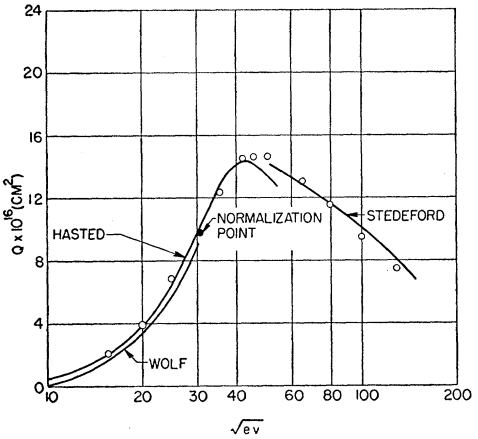

FIG. 2. Relative cross section for slow-ion formation in $p+A$ collisions, normalized at 960 ev.

values of the cross section as presented in the next section.

Our treatment of the ion signal as arising solely through the charge-exchange process (i.e., neglecting those slow ions formed through ionization) would be expected to show itself on our curves of relative cross section. Figures 2 and 3, showing our curves of relative cross section for production of slow ions compared with the results of other experimenters on charge exchange only, demonstrate the extent to which neglect of ionization effects introduces error into all measurements presented in this paper. It seems likely that the $p+A$ cross section of Fig. 2, where the data were normalized to fit Hasted's results, agrees with Stedeford's curve because of formation of argon ions through ionization. In Fig. 3, showing the $p+H_2$ collision results of ourselves and others, normalization at 1800 ev, where

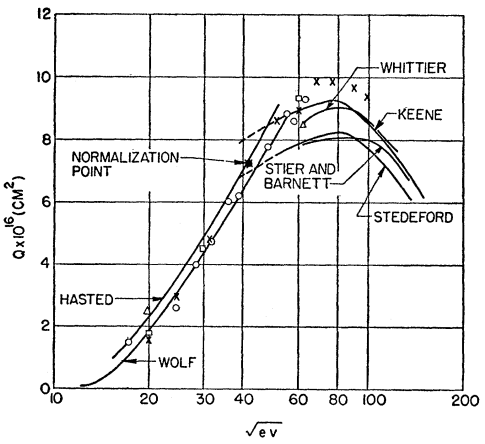

FIG. 3. Relative cross section for slow-ion formation in $p+H_2$ collisions, normalized to the value 7.3×10^{-16} cm² at 1800 ev compared with results of measurements of charge-exchange cross section by Wolf,[8] Keene,[7] Hasted,[6] Stedeford,[6] Whittier,[10] and Stier and Barnett.[11] Different symbols at experimental points are indicative of different runs.

ionization effects should be quite small, puts our higher energy points above the curves of other workers by amounts suggestive of ionization cross-section values. Indeed, a major reason for our selection of 1800 ev as our primary calibration point for determination of absolute cross sections is that, at this energy, ionization must be quite a small effect compared to charge exchange in all reactions studied in these experiments.

IV. RESULTS

The following results were obtained in the determination of absolute values for charge-exchange cross sections.

The (2,2) reaction.—Because of the wide disagreement between Wolf,[8] Hasted,[6,9] Stedeford,[6] and Keene[7] as to the absolute value of the cross section for the (2,2) reaction, it was of interest to measure relative values of the (1,2) and (2,2) reactions at the same energy. Doing this and calibrating on the (1,2) reaction cross

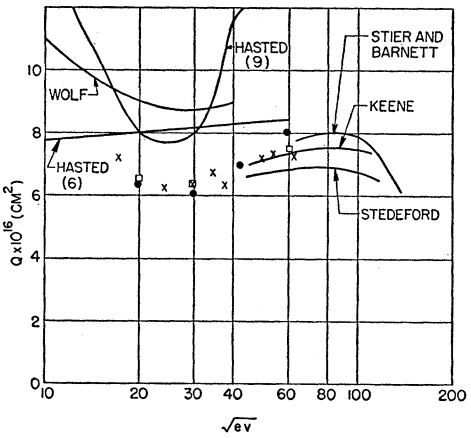

FIG. 4. Cross section for slow-ion formation in collisions between H_2^+ and H_2. Experimental points are normalized to $p+H_2$ results at 1800 ev.

section at 1800 ev, the resulting (2,2) points shown in Fig. 4 were obtained.

The (1,1) reaction.—The proton-hydrogen-atom cross section obtained in our measurements is presented as curve C in Fig. 5, which also shows the calibrating (1,2) reaction (curve A) and the (2,2) reaction (curve B) as determined by ourselves. Individual experimental points are shown to indicate the degree of reproducibility in the experiment at various energies; the probable error shown at 1800 ev (i.e., at 42.5) results from a statistical analysis made with the large amount of data at this point. This probable error does *not* include the uncertainty in the value of the calibrating point, i.e., the cross section for the (1,2) reaction at 1800 ev whose value was taken as 7.3×10^{-16} cm². The reader is again cautioned that our (1,1) curve must be high by amounts which are unknown but which must be less, and are probably substantially less, than

3×10^{-16} cm^2 at low energies and 2×10^{-16} cm^2 at high energies. This correction arises from the unmeasurable effects of ionization and incomplete determination of the slow ions produced in the collisions.

Curves D and E are theoretical curves for the (1,1) process. Curve D is a Born approximation calculation carried out by Bates and Dalgarno,[13] and curve E is the calculation by Dalgarno and Yadav[14] using the method of perturbed stationary states discussed by Bates, Massey, and Stewart.[15] This method formulates the entire problem in terms of molecular-ion wave functions.

As would be expected using the Born approximation, agreement between theory and experiment should be found only at high energies. At lower energies the theoretical values should become too large. It is interesting to note that in our electron-hydrogen-atom collision measurements on ionization[2] and excitation of Lyman alpha radiation,[3] Born approximation calculations appear correct above about 250 ev. In the proton-hydrogen-atom charge-exchange reaction, the threshold proton energy for validity of the Born approximation is about 10 000 ev. Since both these threshold energies correspond to a velocity of about 9×10^{-8} cm/sec, it appears reasonable to generalize that for the Born approximation to be completely reliable, the velocity of the impinging charged particle must be about four times the orbital electron velocity.

In regard to the theory of the p+H charge-exchange reaction, Professor Bates comments that the extent of disagreement between the Born approximation predictions and the experimental results "is associated with the very large magnitude of the cross section (due to the resonance); thus in the Born approximation the reaction

$$H^+ + H \rightarrow H + H^+ \qquad (A)$$

is taken into account, but the inverse reaction

$$H + H^+ \rightarrow H^+ + H \qquad (B)$$

is ignored, and the effect of this inverse reaction is very pronounced since, in effect, the population of the state represented by the right-hand side of (A) and therefore the left-hand side of (B) is very high. In the perturbed stationary state method the coupling due to this back reaction is taken into account (and in the case of resonance is more important than the use of molecular wave functions).[16]"

The remarkable agreement between our measured values and the perturbed stationary state calculations of Dalgarno and Yadav[14] constitutes a very strong recommendation for more extensive use of this approximation in low-energy heavy-particle collision processes.

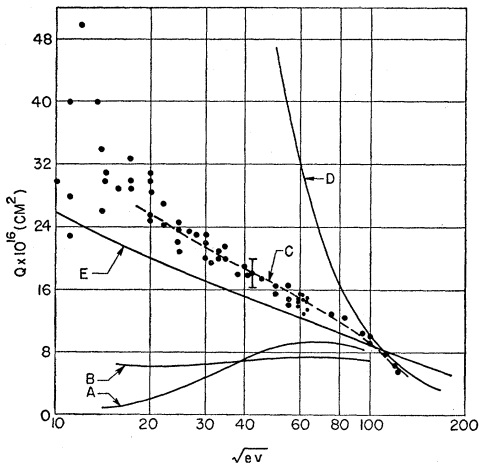

FIG. 5. Cross section for production of slow protons in p+H collisions (curve C) compared to charge-exchange cross sections for $p+H_2 \rightarrow H+H_2^+$ (curve A) experimental; $H_2^+ + H_2 \rightarrow H_2 + H_2^+$ (curve B) experimental; $p+H \rightarrow H+p$ (curve D) theoretical (Bates and Dalgarno); $p+H \rightarrow H+p$ (curve E) theoretical (Dalgarno and Yadav).

The (2,1) reaction.—This reaction was of interest primarily because it is the inverse of the $p+H_2$ collision process. As Fig. 6 demonstrates, the relations between the two inverse reactions are as expected on the basis of the near-adiabatic theory of nonresonant charge-exchange processes.[6,17]

V. EXPERIMENTS USING DEUTERIUM

As stated in the introduction, one of the major motives in our experimental program on atomic collisions is to provide experimental values for cross sections of interest in understanding controlled thermonuclear devices. In all electron-hydrogen-atom collision processes, it makes no difference whether the target is

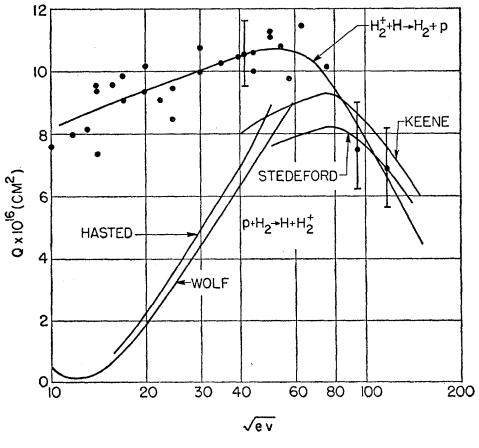

FIG. 6. Comparison of cross sections for inverse processes $p+H_2 \rightleftharpoons H+H_2^+$. Calibration was at 1800 ev.

[13] D. R. Bates and A. Dalgarno, Proc. Phys. Soc. (London) **A66**, 972 (1953).
[14] A. Dalgarno and H. N. Yadav, Proc. Phys. Soc. (London) **A66**, 173 (1953).
[15] Bates, Massey, and Stewart, Proc. Roy. Soc. (London) **A216**, 437 (1953).
[16] D. R. Bates (private communication).
[17] H. S. W. Massey, Repts. Progr. Phys. **12**, 248 (1949).

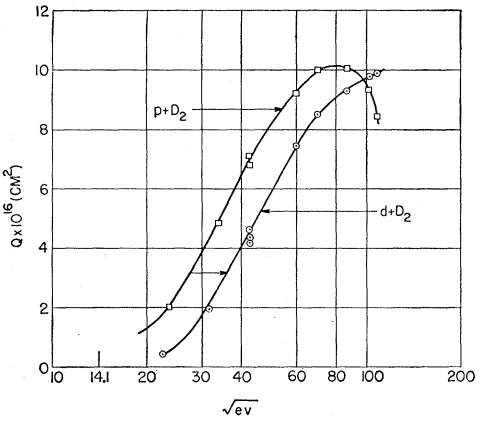

FIG. 7. Comparison of $p+D_2$ and $d+D_2$ charge-exchange reactions, showing shift of energy for given cross-section value expected on basis of difference of velocity of the two ions for the same energy.

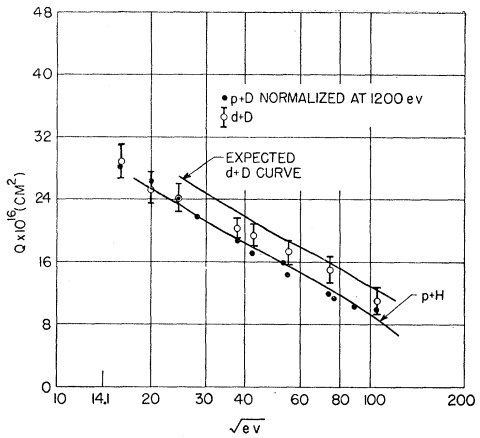

FIG. 8. Comparison of $p+D$ and $d+D$ charge-exchange reactions, showing observed shift and shift expected on basis of difference of velocity of the two ions for the same energy.

a hydrogen atom or a deuterium atom. The only differences between the two types of collision are a negligibly small correction in the reduced masses of the electrons and an equally negligible correction in transferring from center-of-mass to laboratory coordinates.

However, when the target particle is an ion, the cross section for any collision at a given ion energy would be expected to depend on whether the ion is a proton or a deuteron. Although there is presumably no change in the forces acting during the collision, the time during which the interaction takes place will depend on the ion mass.

If the collision cross section depends only on the forces involved and the velocity of the incident ion, the relation between the cross sections for proton and deuteron collisions against the same target system should be very simple. The entire cross-section curve for the deuteron collision should be shifted toward high energies. Using coordinates where the abscissa is the logarithm to the base 10 of $(ev)^{\frac{1}{2}}$, such as we have used, the appropriate shift is a constant 0.15 of a cycle for all energies.

To check this expected shift with ion species, experiments were conducted with deuterium gas (D_2) in the furnace and with ion beams of protons and deuterons. Using the same neutral beam and switching ion types for the same ion energy (by changing the analyzing magnetic field) gives direct measurements of the ratio of cross sections for proton and deuteron collisions against either D or D_2, at the same energy, by taking the ratio of the signals per unit ion current.

Actually, a slight experimental complication arose because the deuteron beam contained some H_2^+ ions. This occurred because the ion source used water vapor for proton production and heavy-water vapor for deuteron production. Since the changeover for ions involved the replacing of gases in the ion source and had to be made expeditiously in order to ensure that the conditions of the neutral deuterium beam remained constant for both types of ions, and since water vapor is a very persistent contaminant, the gas in the ion source was actually a mixture of water and heavy-water vapors at all times. Although there is no question as to the purity of the proton beam (because any other ions are automatically rejected by the ion-beam analyzing magnet), the deuteron beam was contaminated with H_2^+ ions formed from residual light-water vapor in the ion source.

To estimate the amount of H_2^+ ions in the deuteron beam, the following procedure was used. Ion currents of mass 1, 2, and 4 (I_1, I_2, and I_4, respectively) were measured. Assuming (1) that C, the ratio of molecular ion to atomic ion currents, is the same for light and heavy water vapor, (2) that I_1 is a pure proton current, and (3) that I_4 is a current of D_2^+ ions only, then the current at the mass-2 peak is given by

$$I_2=I_{H_2^+}+I_d=CI_1+I_4/C. \tag{7}$$

The currents at the mass-2 peak due to H_2^+ ions and deuterons are, respectively,

$$I_{H_2^+}=CI_1,$$

and

$$I_d=I_4/C,$$

where

$$C=[I_2-(I_2^2-4I_1I_4)^{\frac{1}{2}}]/2I_1. \tag{8}$$

Thus, the signal, $A(2,D)$, found when the mass-2 ion beam crosses the deuterium atom beam is given by

$$\begin{aligned} A(2,D) &\propto I_dQ(d,D)+Q(H_2^+,D)I_{H_2^+}, \\ &=I_2Q(d,D)+[Q(H_2^+,D)-Q(d,D)]I_{H_2^+}, \\ &=Q(d,D)[I_2-CI_1]+Q(H_2^+,D)CI_1, \end{aligned} \tag{9}$$

where $Q(d,D)$ is the cross section for the $d+D$ reaction and $Q(H_2^+,D)$ is that for the H_2^++D reaction. After ten minutes following change-over from light water to heavy water, C was found to take a steady-state value of 0.15 ± 0.01, and I_1/I_2 became equal to 0.37 ± 0.01, which also held steady for the duration of the measurements, so that CI_1/I_2 became 0.055 ± 0.004. Thus the

signal per unit mass-2 ion current becomes, from (9),

$$S(2,\mathrm{D})=A(2,\mathrm{D})/I_2\gtrsim[0.945Q(d,\mathrm{D}) +0.055Q(\mathrm{H_2^+},\mathrm{D})]. \quad (10)$$

Since the signal per unit ion current found when the proton beam crossed the deuterium atom beam is given by

$$S(1,\mathrm{D})=A(1,\mathrm{D})/I_1\propto Q(p,\mathrm{D}),$$

and the constant of proportionality is the same for the same neutral beam and geometry, we have

$$\frac{Q(d,\mathrm{D})}{Q(p,\mathrm{D})}=\frac{1}{0.945}\left[\frac{S(2,\mathrm{D})}{S(1,\mathrm{D})}-0.055\frac{Q(\mathrm{H_2^+},\mathrm{D})}{Q(p,\mathrm{D})}\right]. \quad (10a)$$

Similarly, when the neutral beam consists of D_2 rather than deuterium atoms, an identical argument yields the analogous formula

$$\frac{Q(d,\mathrm{D_2})}{Q(p,\mathrm{D_2})}=\frac{1}{0.945}\left[\frac{S(2,\mathrm{D_2})}{S(1,\mathrm{D_2})}-0.055\frac{Q(\mathrm{H_2^+},\mathrm{D_2})}{Q(p,\mathrm{D_2})}\right]. \quad (10b)$$

These two formulas were used in evaluating the cross-section ratios. The values for $Q(p,\mathrm{D})$, $Q(p,\mathrm{D_2})$, $Q(\mathrm{H_2^+},\mathrm{D})$, $Q(\mathrm{H_2^+},\mathrm{D_2})$ were taken as the values previously determined when the neutral beam consisted of light hydrogen atoms and molecules (as shown in Figs. 5, 3, 6, and 4, respectively) after it had been ascertained that the curves of relative cross section were the same whether light or heavy hydrogen was used in the neutral beam.

The results of the measurements comparing proton and deuteron bombardment of the same neutral beam are shown in Figs. 7 and 8, where the data were handled according to Eqs. (10). When the deuterium molecule was the target (Fig. 7), the shift of the two curves along the energy axis could hardly have been in better agreement with the theoretical considerations presented above.

When the target system was the deuterium atom (Fig. 8), the expected shift was not observed. We cannot at the present time resolve the dilemma presented by the disagreement between the very convincing simple theoretical arguments and the equally convincing direct experimental data.

ACKNOWLEDGMENTS

We are indebted to a number of our colleagues, especially Dr. Samuel P. Cunningham and Dr. Donald W. Kerst, for their interest in these experiments and discussions of them. We are especially indebted to Professor D. R. Bates of Queen's University, Belfast, for his comments on the relation of these measurements to theory.

As always, the assistance of Miss Eugenia Rossell in the operation of the atomic beam apparatus has greatly accelerated the progress of these experiments.

PHYSICAL REVIEW VOLUME 112, NUMBER 4 NOVEMBER 15, 1958

Electron Spin Resonance of Atomic and Molecular Free Radicals Trapped at Liquid Helium Temperature*

C. K. Jen, S. N. Foner, E. L. Cochran, and V. A. Bowers
Applied Physics Laboratory, The Johns Hopkins University, Silver Spring, Maryland

(Received June 17, 1958)

Electron spin resonance spectra of H, D, N, and CH_3 trapped in solid matrices at liquid helium temperature have been observed and interpreted. The effect of the matrix field on the resonance properties of the radicals has been investigated by depositing the radicals in matrices with different binding energies. The effect of the matrix on the g factor is extremely small in all cases. The deviation of the hyperfine coupling constant from the free-state value increases in a systematic way with increase in binding energy of the matrix, the percentage deviations being small for H, D, and CH_3 but rather large for the case of N. The widths and shapes of the spectral lines are discussed in terms of dipolar broadening, spin-lattice relaxation, anisotropic broadening, rate of passage and the modulation parameters used for observation.

Complex spectra, not adequately identified, have been observed from discharges in hydrogen and hydrogen-oxygen systems. Deductive evidence for an HO_2 resonance spectrum is presented.

The stable molecular free radicals O_2, NO, and NO_2 have been studied. Only NO_2 yielded a positive result. Resonances for oxygen and chlorine atoms have been sought but not observed. It is suggested that radical species with orbital angular momenta may escape spin resonance observation because of matrix field anisotropy and that radical species with an even number of electrons may be unobservable because of crystalline field splitting resulting in a singlet ground level.

I. INTRODUCTION

FREE radicals trapped in solid media can be generated *in situ* by irradiation (uv, x-ray, γ-ray, electron, neutron, etc.) or can be generated in the gaseous state and subsequently deposited in a suitable matrix. While the technique of stabilizing free radicals by isolating them in a rigid matrix is not new[1] and many frozen chemical systems have been examined

* This work supported by Bureau of Ordnance, Department of the Navy.

[1] G. N. Lewis and D. Lipkin, J. Am. Chem. Soc. **64**, 2801 (1942).